The Nonribosomal Peptide Synthetase HMWP2 Forms a Thiazoline Ring during Biogenesis of Yersiniabactin, an Iron-Chelating Virulence Factor of *Yersinia pestis*†

Amy M. Gehring,[§,||] Ichiro Mori,[§,||] Robert D. Perry,[⊥] and Christopher T. Walsh*[,§]

Department of Biological Chemistry and Molecular Pharmacology, Harvard Medical School, 240 Longwood Avenue, Boston, Massachusetts 02115, and Department of Microbiology and Immunology, University of Kentucky, Lexington, Kentucky 40536-0084

Received May 27, 1998; Revised Manuscript Received June 30, 1998

ABSTRACT: Pathogenic *Yersinia* species have been shown to synthesize a siderophore molecule, yersiniabactin, as a virulence factor during iron starvation. Here we provide the first biochemical evidence for the role of the *Yersinia pestis* high molecular weight protein 2 (HMWP2), a nonribosomal peptide synthetase homologue, and YbtE in the initiation of yersiniabactin biosynthesis. YbtE catalyzes the adenylation of salicylate and the transfer of this activated salicyl group to the N-terminal aryl carrier protein domain (ArCP; residues 1−100) of HMWP2. A fragment of HMWP2, residues 1−1491, can adenylate cysteine and with the resulting cysteinyl-AMP autoaminoacylate the peptidyl carrier protein domain (PCP1; residues 1383−1491) either in cis or in trans. Catalytic release of hydroxyphenylthiazoline carboxylic acid (HPT-COOH) and/or *N*-(hydroxyphenylthiazolinylcarbonyl)cysteine (HPT-cys) is observed upon incubation of YbtE, HMWP2 1−1491, L-cysteine, salicylate, and ATP. These products presumably arise from nucleophilic attack by water or cysteine of a stoichiometric hydroxyphenylthiazolinylcarbonyl-S-PCP1-HMWP2 intermediate. Detection of the heterocyclization capacity of HMWP2 1−1491 implies salicyl-transferring and thiazoline-forming activity for the HMWP2 condensation domain (residues 101−544) and is the first demonstration of such heterocyclization ability in a nonribosomal peptide synthetase enzyme.

The virulence of the pathogenic yersiniae, including *Yersinia pestis* which causes bubonic plague (*1*) and the food-borne pathogen *Yersinia enterocolitica* (*2*), has been clearly correlated with the amount of iron available to these organisms. The ability to obtain iron from the host has been shown to affect the virulence of many bacterial species (*3*), with the production, secretion, and reuptake of siderophores, small molecules with high affinity for ferric iron (*4*), being a common microbial strategy for iron acquisition. Secretion of the siderophore molecule yersiniabactin (or yersiniophore) has been detected in mouse-lethal strains of *Y. enterocolitica* (*5*, *6*) as well as in human isolates (*7*). The structure of yersiniabactin was recently determined independently by two groups (*8*, *9*) and contains a phenolic group (presumably derived from salicylate) and three five-membered heterocycles of the thiazole group (presumably derived from cysteine), two at the dihydro oxidation state (thiazoline) and one at the tetrahydro oxidation state (thiazolidine), as potential high-affinity iron ligands (Scheme 1). Yersiniabactin isolation and characterization from *Y. pestis* indicates that this plague-causing organism synthesizes the same siderophore molecule (R. D. P., L. E. DeMoll, manuscript in preparation). Several other bacterial siderophores have

Scheme 1

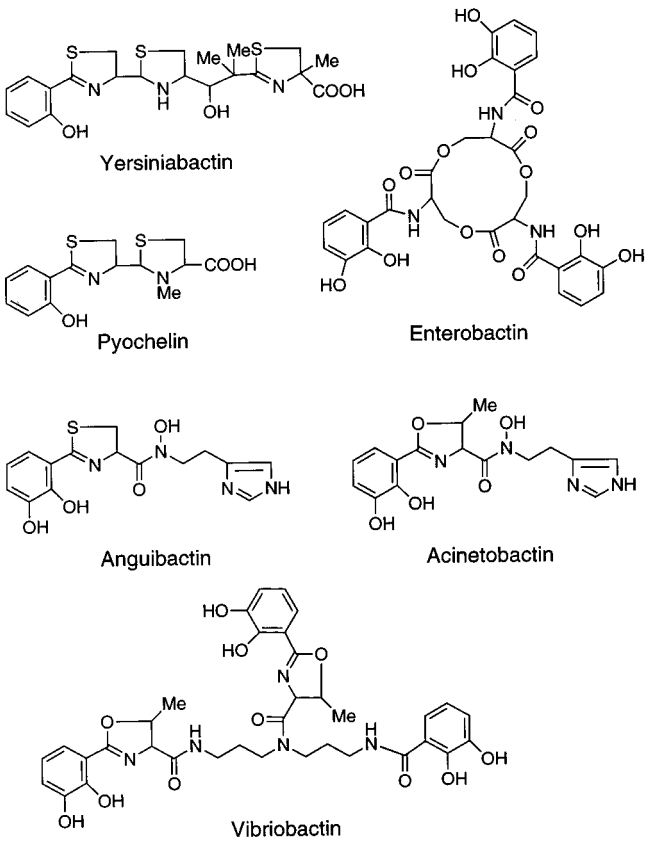

structures similar to yersiniabactin including pyochelin from *Pseudomonas aeruginosa* (*10*), anguibactin from *Vibrio*

† This work was supported by National Institutes of Health grant R01 AI042738 to C.T.W. and R.D.P. A.M.G. is a Howard Hughes Medical Institute Predoctoral Fellow. I. M. is a visiting scientist from Novartis Japan.

* Author to whom correspondence should be addressed.
§ A.M.G. and I.M. contributed equally to this work.
|| Harvard Medical School.
⊥ University of Kentucky.

S0006-2960(98)01257-4 CCC: $15.00
Published on Web 07/29/1998

anguillarum (*11*), acinetobactin from *Acinetobacter baumannii* (*12*), and vibriobactin from *Vibrio cholerae* (*13*) (Scheme 1).

A high pathogenicity island has been described in the chromosomes of highly pathogenic *Y. pestis*, *Y. enterocolitica*, and *Y. pseudotuberculosis* strains (*14*−*17*) which contains a cluster of iron-repressible genes involved in the synthesis, regulation, and uptake of yersiniabactin (*18*). This locus has been sequenced in *Y. pestis* (*19, 20*; R. D. P., personal communication) and *Y. enterocolitica* (*21*−*23*) and includes the yersiniabactin receptor gene *psn* (*fyuA* in *Y. enterocolitica*) as well as the putative yersiniabactin biosynthetic genes *irp2*, *irp1*, *ybtE* (*irp5*), and *ybtT* (*irp4*). The *irp2* and *irp1* genes encode the 230 kDa high molecular weight protein 2 (HMWP2)[1] (*22*) and the 350 kDa high molecular weight protein 1 (HMWP1) (*23*), respectively, which show considerable homology to nonribosomal peptide synthetases, polyketide synthases, and siderophore synthetases, in particular the *Escherichia coli* enterobactin synthetase. YbtE is 61% similar to *E. coli* EntE, the 2,3-dihydroxybenzoate adenylating and loading enzyme in enterobactin biosynthesis, and YbtT is 59% similar to the thioesterase-like protein associated with anguibactin biosynthesis (*20*). Mutation of the *irp1*, *irp2*, or *ybtE* genes in *Y. pestis* eliminates siderophore production by these strains (*20*).

We have recently characterized the *E. coli* enterobactin synthetase (*24, 25*), and its organization provides a blueprint for studies of the yersiniabactin synthetase (Figure 1). The synthesis of enterobactin, a cyclic trimeric lactone of *N*-(2,3-dihydroxybenzoyl)serine (DHB-ser) (Scheme 1), requires the EntB, -E, and -F proteins. EntE adenylates 2,3-dihydroxybenzoate (DHB) and then catalyzes transfer of the dihydroxybenzoyl group to the phosphopantetheine (Ppant) cofactor of the aryl carrier protein (ArCP) domain of EntB (*24*). The acylated EntB then serves as an aryl donor substrate for amide bond formation by the multidomainal EntF with DHB-ser formation on the Ppant cofactor of the peptidyl carrier protein (PCP) domain of EntF indicated (*25*). Ester bond formation between three DHB-ser units completes enterobactin biosynthesis. There is a close correspondence between the domain organization of the three protein EntB, -E, and -F system and the two protein YbtE, HMWP2 pair (Figure 1). YbtE is a close homologue of EntE (*20*), and the N-terminal 100 residues of HMWP2 show 27% identity to the EntB ArCP domain. HMWP2 also includes condensation, amino acid adenylation, and PCP domains analogous to EntF which could give a salicyl-cys-Ppant-PCP intermediate. It therefore seemed likely that YbtE and HMWP2 might initiate yersiniabactin biogenesis by activating salicylate and the first two of the three cysteine precursors which become thiazoline/thiazolidine rings in the final yersiniabactin structure (Scheme 1). HMWP1 would presumably complete the synthesis of the yersiniabactin molecule.

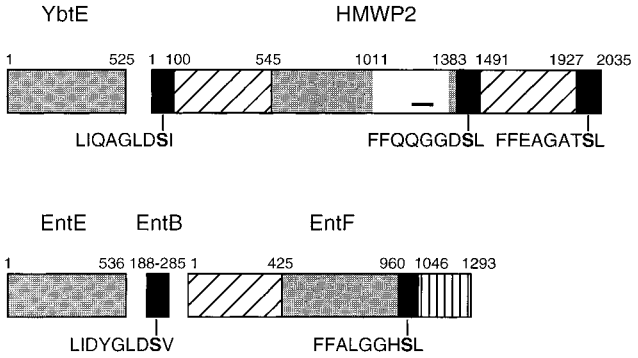

FIGURE 1: Domain organization of the yersiniabactin synthetase compared to the enterobactin synthetase. Yersiniabactin biosynthesis is initiated by the salicylate-adenylating enzyme YbtE and the multidomainal HMWP2. HMWP2 has three carrier protein domains (black): an N-terminal ArCP domain (residues 1−100), an internal PCP domain (residues 1383−1491), and a C-terminal PCP domain (1927−2035). The local sequence surrounding the putative phosphopantetheinylated serine residue (bold) in these domains is noted. The cysteine adenylation domain of HMWP2 (gray, residues 545−1382) is interrupted between motifs A8 and A9 by a putative methyltransferase domain (white, residues 1011−1347), with the region of methyltransferase homology denoted with a dark line. HMWP2 additionally has two condensation/cyclization domains (diagonal stripe, residues 101−544, 1492−1926). The enterobactin synthetase has a similar organization with the DHB-adenylating enzyme EntE loading the ArCP domain of EntB. The DHB-loaded EntB is the substrate for the multidomainal EntF possessing condensation (diagonal stripe), serine adenylation (gray), PCP (black) and thioesterase (vertical stripe) domains.

In this work, we biochemically demonstrate the roles of the *Y. pestis* YbtE and HMWP2 enzymes in yersiniabactin biosynthesis. YbtE adenylates salicylate and then transfers the salicyl group to the N-terminal ArCP domain of HMWP2. A fragment of HMWP2 (residues 1−1491) can catalyze the adenylation of cysteine, the transfer of this activated cysteine group to the Ppant cofactor of a PCP domain, and the formation of the hydroxyphenylthiazoline carboxylate (HPT-COOH) intermediate in yersiniabactin biosynthesis. This is the first enzymological characterization of yersiniabactin biosynthetic enzymes as well as the first demonstration of an enzyme's ability to catalyze the five-membered ring heterocyclization that characterizes a large class of oxazole and thiazole-containing nonribosomal peptide-based natural products.

MATERIALS AND METHODS

Overproduction and Purification of YbtE. The *Y. pestis ybtE* gene was amplified by polymerase chain reaction (PCR) from pSDR498.4 (*26*) using the *Pfu* polymerase (Stratagene), primer 1 (5′-ACTCCATATGAATTCTTCCTTTGAATC-3′) and primer 2 (5′-GATGAAGCTTGTTGTGAGTCCCTG TAAG-3′) (Integrated DNA Technologies, Inc.; restriction sites underlined). The PCR product was cloned into the *Nde*I/*Hin*dIII sites of the pPROEX-1 vector (Life Technologies) to give pH6YBTE1. The fidelity of the cloned insert

[1] Abbreviations: ArCP, aryl carrier protein; CoASH, coenzyme A; DHB, 2,3-dihydroxybenzoate; DHB-ser, *N*-(2,3-dihydroxybenzoyl)-serine; DTT, DL-dithiothreitol; FAB-MS, fast atom bombardment mass spectrometry; HPLC, high-performance liquid chromatography; HPT-COOH, 4,5-dihydro-2-(2-hydroxyphenyl)-4-thiazolecarboxylic acid; HPT-cys, *N*-{[2-(2-hydroxyphenyl)]-4,5-dihydrothiazole-4-carbonyl}-cysteine; HPTT-COOH, 2′-(2-hydroxyphenyl)-4,5,4′,5′-tetrahydro-2,4′-bithiazolyl-4-carboxylic acid; HRMS, high-resolution mass spectrometry; HMWP, high molecular weight protein; IPTG, isopropyl β-D-thiogalactopyranoside; LC-MS, liquid chromatography−mass spectrometry; MES, 2-[*N*-morpholino]ethanesulfonic acid; NMR, nuclear magnetic resonance spectroscopy; PCP, peptidyl carrier protein; PCR, polymerase chain reaction; PP_i, pyrophosphate; Ppant, 4′-phosphopantetheine; PPTase, phosphopantetheinyl transferase; sal, salicylate; SDS−PAGE, sodium dodecyl sulfate−polyacrylamide gel electrophoresis; TCA, trichloroacetic acid.

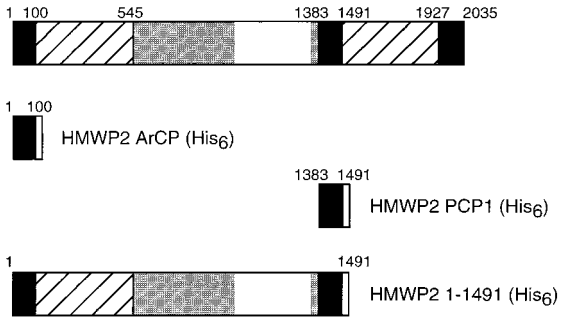

FIGURE 2: The HMWP2 fragments used in this study. All fragments were expressed as C-terminal hexahistidine-tagged fusions (white box). The HMWP2 ArCP (residues 1−100), HMWP2 PCP1 (residues 1383−1491), and HMWP2 1−1491 were all overproduced in *E. coli* and purified by nickel chelate chromatography.

was confirmed by DNA sequencing. Cloning into the *Nde*I site of pPROEX1 appends a 24 amino acid sequence, including a hexahistidine tag, to the N-terminus of the overproduced YbtE protein.

Cultures of *E. coli* strain BL21(DE3) transformed with pH6YBTE1 (2 L, 2 × YT media, 50 μg/mL ampicillin) were grown at 37 °C to an optical density (600 nm) of 0.8 and then induced with 1 mM isopropyl β-D-thiogalactopyranoside (IPTG). Cells were harvested after 4 h, and the cell paste was resuspended in buffer A (20 mM Tris-HCl, pH 7.9, 0.5 M NaCl) containing 5 mM imidazole. Cells were lysed by two passages through a French pressure cell at 15 000 psi, and the lysate was clarified by centrifugation (27 000 × *g*). The protein was purified from this lysate by nickel chelate chromatography over His·Bind resin (5 mL column) according to the manufacturer's specifications (Novagen). Fractions containing YbtE as judged by SDS-polyacrylamide gel electrophoresis (SDS−PAGE) were pooled and dialyzed against 25 mM Tris-HCl, pH 8.0, 10 mM $MgCl_2$, 5 mM DTT, 10% glycerol, flash frozen in liquid nitrogen, and stored at −80 °C. The protein concentration of the purified enzyme preparation was determined using the calculated extinction coefficient (*27*) for the absorbance of YbtE at 280 nm: 54 420 M^{-1} cm^{-1}.

Overproduction and Purification of the HMWP2 ArCP and PCP1 Fragments. The *Y. pestis irp2* ArCP gene fragment (corresponding to residues 1−100 of the HMWP2 protein; Figure 2) was amplified from pPROEX-irp2-1 (R. D. P., unpublished) by PCR using *Pfu* polymerase, primer 3 (5′-GAATTCCATATGATTTCTGGCGCA-3′) and primer 4 (5′-TGACCGCTCGAGCAAGCTTTCTTCTTCCGC-3′). Because of the design of primer 4, residues 99 and 100 of the HMWP2 ArCP fragment are mutated from TP to SL in the overproduced protein. The PCR product was cloned into the *Nde*I/*Xho*I sites of pET22b (Novagen) to give the plasmid pET22b-irp2ArCP. This plasmid directs overproduction of the ArCP as a histidine tag fusion with the amino acid sequence LEHHHHHH appended to the C-terminus. The *Y. pestis irp2* PCP1 gene fragment (corresponding to residues 1383−1491 of the HMWP2 protein; Figure 2) was amplified and cloned into pET22b in the same manner except that the template was pIRP2 (*20*) and primer 5 (5′-GAATTC-CATATGATTGACTACCAGGCGCTGA-3′) and primer 6 (5′-TGACCGCTCGAGTTCTTCAGGAGAGTGG-3′) were used to give the plasmid pET22b-irp2PCP1. Because of the design of primer 6 (which was based on the *Y. enterocolitica irp2* sequence), residue 1491 of PCP1 is mutated from D to E. The DNA sequences of the pET22b-irp2ArCP and pET22b-irp2PCP1 inserts were confirmed by sequencing (Dana Farber Molecular Biology Core Facility, Boston, MA).

Overproduction and purification of HMWP2 ArCP and PCP1 were as described above for YbtE except that culture growth after induction with IPTG was for 3 h. Fractions containing ArCP or PCP1 were pooled and dialyzed against 50 mM Tris-HCl, pH 8.0, 2 mM DTT, 5% glycerol, flash frozen in liquid nitrogen, and stored at −80 °C. The concentration of the purified HMWP2 ArCP preparation was determined using the Bio-Rad Protein Assay reagent. The concentration of the PCP1 preparation was determined using the calculated extinction coefficient (*27*) for the absorbance of the protein at 280 nm: 8250 M^{-1} cm^{-1}.

Overproduction and Purification of HMWP2 1−1491. The *Y. pestis irp2* gene fragment corresponding to residues 1−1491 of HMWP2 was cloned into pET22b in two steps. First, the gene fragment corresponding to residues 1−1061 of HMWP2 was amplified by PCR using the *Pfu* polymerase, pIRP2 (*20*) as the template, primer 3, and primer 7 (5′-TGACCGCTCGAGGTGACCCGGCTTCAGTTT-3′). This PCR product was cloned into the *Nde*I/*Xho*I sites of pET22b to give pET22b-irp2/1−1061. The pIRP2 plasmid was used as the template in another PCR reaction using primer 8 (5′-CTCGGCTGCTACTGGCCAGACGGCAC-3′) (*Msc*I site underlined) and primer 6. This PCR product was digested with *Msc*I and *Xho*I and cloned into pET22b-irp2/1−1061 to give pET22b-irp2/1−1491. The DNA sequence of the pET22b-irp2/1−1491 insert was confirmed by sequencing (Dana Farber Molecular Biology Core Facility, Boston, MA).

HMWP2 1−1491 was overproduced and purified several times, each with a slightly different protocol, to provide material for the experiments described in this manuscript. Although this protein is overproduced with a C-terminal hexahistidine tag, it did not bind well to the nickel chelate column necessitating changes to the manufacturer's protocol. A representative overproduction/purification procedure is described here. Cultures of *E. coli* strain BL21(DE3) transformed with pET22b-irp2/1−1491 (3 L, LB, 50 μg/mL ampicillin) were grown at 30 °C to an optical density of 1.2. The temperature was lowered to 25 °C, and the cultures were induced with 1 mM IPTG. Cells were harvested after an additional 4 h of growth, the cell paste was resuspended in 20 mM Tris-HCl, pH 7.9, 200 mM NaCl, and cells were lysed by passage through a French pressure cell as described above. The clarified lysate was applied to a 5 mL His·Bind column at a flow rate of 0.8 mL/min. The column was washed successively with the following: 15 mL of buffer A; 35 mL of buffer A containing 5 mM imidazole; 10 mL of buffer A containing 32.5 mM imidazole; 20 mL of buffer A containing 60 mM imidazole. HMWP2 1−1491 was eluted from the column with 12 mL of buffer A containing 204 mM imidazole. As judged by SDS−PAGE, both the 60 mM imidazole wash fractions and the elution fractions contained significant amounts of HMWP2 1−1491. The wash and elution fractions were pooled separately and dialyzed against buffer B (25 mM Tris-HCl, pH 8.0, 2 mM DTT) containing 10% glycerol.

The dialyzed wash and elution fractions were further purified by anion-exchange chromatography on a Q-Sepharose column (2.5 × 10 cm) and a POROS 20 HQ

column (4.6 × 100 mm) for use with the BioCAD SPRINT perfusion chromatography system (PerSeptive Biosystems, Inc.) repectively. For the Q-Sepharose chromatography of the His·Bind wash fractions, the protein was applied to the column (flow rate 2 mL/min) which was then washed with 50 mL of buffer B followed by a 100 mL gradient of 0 to 250 mM KCl (in buffer B). Protein was eluted with a 350 mL gradient of 250 to 650 mM KCl (in buffer B). For the BioCAD chromatography of the His·Bind elution fractions, the protein was applied to the column (flow rate 10 mL/min) which was then washed with 4 column volumes of 10 mM Tris, 10 mM Bis-tris propane, pH 8.0 (buffer C), followed by an 8 column volume gradient of 0 to 250 mM NaCl (in buffer C). Protein was eluted over a 25 column volume gradient from 250 to 500 mM NaCl (in buffer C). Following anion-exchange chromatography, fractions containing HMWP2 1−1491 as judged by SDS−PAGE were pooled, dialyzed against buffer B containing 10% glycerol, flash frozen in liquid nitrogen, and stored at −80 °C. The concentration of the HMWP2 1−1491 preparations was determined using the calculated extinction coefficient (*27*) of this protein at 280 nm: 266 460 M^{-1} cm^{-1}.

Preparation and Purification of Holo-ArCP, Holo-PCP1, and Holo-HMWP2 1−1491. Holo-ArCP covalently modified by attachment of the Ppant cofactor was prepared by incubating the purified apo-ArCP with a phosphopantetheinyl transferase (PPTase), purified *E. coli* EntD (*28*), and coenzyme A (CoASH). The following were incubated at 37 °C for 3.5 h to produce holo-ArCP (4 mL final volume): 75 mM Tris-HCl, pH 7.5, 10 mM $MgCl_2$, 5 mM DTT, 0.4 mM CoASH, 207 μM apo-ArCP, and 1.2 μM EntD. Following reaction, the mixture was dialyzed against buffer A containing 5 mM imidazole. The holo-ArCP was purified by nickel chelate chromatography and stored as described for apo-ArCP. The concentration of the holo-ArCP preparation was determined using the calculated extinction coefficient (*27*) for the absorbance of this protein at 280 nm: 20 910 M^{-1} cm^{-1}. Complete phosphopantetheinylation of the holo-ArCP preparation was confirmed using the radioassay for [^{3}H]Ppant incorporation described below.

Holo-PCP1 was prepared by incubating the purified apo-PCP1 with purified Sfp, a phosphopantetheinyl transferase from *Bacillus subtilis* (*28*) and CoASH. The following were incubated at 37 °C for 1 h (4 mL final volume): 75 mM MES/sodium acetate, pH 6.0, 10 mM $MgCl_2$, 5 mM DTT, 1 mM CoASH, 150 μM apo-PCP1, and 0.4 μM Sfp. Some protein precipitated over the course of this reaction and was removed by centrifugation. The holo-PCP1 was purified from the clarified reaction mixture on the POROS 20 HQ anion-exchange column. Holo-PCP1 was loaded on the column (flow rate 10 mL/min) which was then washed with 4 column volumes of buffer C. A 30 column volume gradient of 0−500 mM NaCl (in buffer C) was then applied. As determined by SDS−PAGE, most of the holo-PCP1 flowed through the column. These flow-through fractions were pooled, dialyzed, and stored as described for apo-PCP1.

Holo-HMWP2 1−1491 was prepared by incubation of purified apo-HMWP2 1−1491 with purified Sfp. The following were incubated at 37 °C for 30 min (3 mL final volume): 75 mM MES/sodium acetate, pH 6.5, 10 mM $MgCl_2$, 5 mM DTT, 0.4 mM CoASH, 10 μM apo-HMWP2 1−1491, and 0.4 μM Sfp. Some protein precipitated over the course of the reaction and was removed by centrifugation. The holo-HMWP2 1−1491 was purified from the clarified reaction mixture using the POROS 20 HQ anion-exchange column and the same program as described for the holo-PCP1 purification. HMWP2 1−1491 eluted about midway through the gradient step as determined by SDS−PAGE. Fractions containing holo-HMWP2 1−1491 were handled as above for apo-HMWP2 1−1491 except that 50 mM Tris-HCl was used in the dialysis buffer.

Assay for the Phosphopantetheinylation of ArCP and PCP Domains. The trichloroacetic acid (TCA) precipitation radioassay which measures phosphopantetheinyl transferase activity as attachment of [^{3}H]P_{pant} from [^{3}H]CoASH to the carrier protein substrate was carried out as described previously (*24, 28*). For the K_m determination of the apo-HMWP2 ArCP for EntD, varying concentrations of the apo-ArCP were incubated with 75 mM Tris-HCl, pH 7.5, 10 mM $MgCl_2$, 5 mM DTT, 150 μM [^{3}H]CoASH (200 Ci/mol, 70% label in Ppant), and 25 nM EntD (100 μL reaction volume, triplicate reactions) at 37 °C for 15 min prior to quenching with TCA.

For autoradiography, substrates (6 μM apo-ArCP, 6 μM apo-PCP1, or 1 μM apo-HMWP2 1−1491) were incubated with and without 0.8 μM EntD as described above. Following TCA precipitation, the protein pellet was dissolved in SDS sample buffer (20 μL) and 1 M Tris base (3 μL) and electrophoresed on a 4−20% Tris-glycine gel (Bio-Rad). For visualization, the gel was stained with Coomassie blue solution, destained, and soaked in Amplify (Amersham) for 25 min. The dried gel was exposed to film for 2 days.

Assays for the Partial Reactions Catalyzed by YbtE

(a) ATP-[^{32}P]PP_i Exchange Activity. The ATP-pyrophosphate (PP_i) exchange assay was performed as described previously (*25*). Reaction mixtures contained (final volume 100 μL, triplicate reactions) 75 mM Tris-HCl, pH 8.8, 10 mM $MgCl_2$, 5 mM DTT, 1 mM sodium [^{32}P]PP_i (9 Ci/mol), salicylate, and ATP. For the determination of the ATP K_m value, 50 μM salicylate was used in each assay. For the salicylate and DHB K_m determinations, 2.5 mM ATP was used. The assay was initiated by the addition of 25 nM YbtE and incubated at 37 °C for 10 min.

(b) Assay for the Acylation of HMWP2 with [^{14}C]-Salicylate. The TCA precipitation radioassay for the YbtE-catalyzed transfer of [^{14}C]salicylate to the holo-HMWP2 fragments was as described for the reaction of EntE with EntB (*24*). For the determination of the K_m of holo-HMWP2 ArCP in the reaction with YbtE, varying concentrations of the holo-ArCP were incubated with 75 mM Tris-HCl, pH 8.8, 10 mM $MgCl_2$, 5 mM DTT, 5 mM ATP, 90 μM [^{14}C]-salicylate (55.5 Ci/mol), and 2.5 nM YbtE (100 μL volume, triplicate reactions) at 37 °C for 5 min prior to quenching with TCA.

For autoradiography, the HMWP2 substrate (6 μM holo-ArCP, 6 μM holo-PCP1, or 1 μM HMWP2 1−1491) was incubated with and without 1 μM YbtE. Reaction mixtures also included (100 μL final volume) 75 mM Tris-HCl, pH 8.0, 10 mM $MgCl_2$, 5 mM DTT, 10 mM ATP, and 90 μM [^{14}C]salicylate (55.5 Ci/mol) and were incubated at 37 °C for 15 min. In one reaction of HMWP2 1−1491 and YbtE, 3 mM L-cysteine was also included. This autoradiograph was prepared as described above. The film was exposed to

the dried gel for 2.5 days prior to development.

Assays for the Partial Reactions Catalyzed by HMWP2 1−1491

(a) ATP-[^{32}P]PP$_i$ Exchange Activity. ATP−PP$_i$ exchange activity for HMWP2 1−1491 was assayed as described previously (*25*). Reaction mixtures (100 μL, triplicate) included 75 mM Tris-HCl pH 8.8, 10 mM $MgCl_2$, 5 mM DTT, 1 mM sodium [^{32}P]PP$_i$ (8 Ci/mol), ATP, L-cysteine, and 30 nM apo-HMWP2 1−1491 and were incubated for 5 min at 37 °C. For the determination of the ATP K_m, varying concentrations of ATP were used while L-cysteine was held at 5 mM. For the L-cysteine K_m determination, ATP concentration was held at 3 mM.

(b) Autoradiography Demonstrating the Aminoacylation of HMWP2 with [^{35}S]-L-Cysteine. For autoradiography, HMWP2 (1 μM) was incubated with [^{35}S]-L-cysteine (0.68 mM, 55.5 Ci/mol) and in some cases holo-ArCP (15 μM) or holo-PCP1 (15 μM). Reaction mixtures also included 75 mM Tris-HCl, pH 8.0, 10 mM $MgCl_2$, 5 mM DTT, and 10 mM ATP and were incubated at 37 °C for 15 min. One reaction contained in addition to holo-HMWP2 1−1491 and [^{35}S]cysteine, 1 μM YbtE, and 1 mM salicylate. The autoradiograph was prepared as described above. The dried gel was exposed to film for 16 days before developing.

Detection and Identification of HMWP2 1−1491 Reaction Products

(a) HPLC Time Course Assay for the Production of HPT-cysteine (HPT-cys). The HPLC assay for the detection of HPT-cys production was conducted as follows: reaction mixtures (500 μL) contained 75 mM Tris-HCl, pH 8.8, 10 mM $MgCl_2$, 5 mM DTT, 1 mM CoASH, 5 mM L-cysteine, 1 mM salicylate, 0.1 μM YbtE, 1 μM EntD, 2 μM apo-HMWP2 1−1491, and 10 mM ATP to initiate the reaction. Prior to the addition of ATP, the reaction mixture was incubated for 10 min at room temperature to allow phosphopantetheinylation of apo-HMWP2 1−1491 by EntD. After the addition of ATP, the reaction mixture was incubated at 37 °C and 50 μL samples were removed at specified times. Each 50 μL sample was acidified to pH ≈1.5 by the addition of 10 μL of 8.5% phosphoric acid. The acidified reaction mixture was washed with 375 μL of ethyl acetate. A portion of the ethyl acetate layer (250 μL) was concentrated under reduced pressure, and the residue was dissolved in 250 μL of 30% acetonitrile/water. Samples of 100 μL were analyzed by HPLC (Waters) on a C18 reverse phase column (VYDAC, 250 × 5 mm) with a detector wavelength of 250 nm and a mobile phase with the following gradient. Mobile phase A: a mixture of formic acid (0.1 mL) and triethylamine (0.2 mL) in water (1 L) (pH 3.3). Mobile phase B: a 4:1 mixture of acetonitrile and mobile phase A. At a flow rate of 1 mL/min, time 0.0 min (90% A), 17.0 min (20% A), and 17.10 min (90% A), and at 1.5 mL/min, time 25.00 min (90% A). (*29*) For the experiments described in Figure 7C, reaction conditions were slightly altered with 1.5 mM cysteine, 1.5 mM salicylate, and 3.6 μM 1−1491 with a 1 h incubation time; reaction components were omitted as indicated.

(b) Isolation of HPT-cys for Mass Spectrometry Analysis. To prepare large quantities of HPT-cys for HPLC purification and mass spectrometry, the following were incubated at 37 °C for 4 h, 75 mM Tris-HCl, pH 8.8, 10 mM $MgCl_2$, 5 mM DTT, 1 mM CoASH, 10 mM ATP, 1.5 mM L-cysteine, 1.5 mM salicylate, 0.1 μM YbtE, 1 μM EntD, and 3.6 μM HMWP2 1−1491, to a final volume of 500 μL. Samples of 20 μL were removed at 1 and 2 h for monitoring the reaction progress by HPLC. The remaining reaction mixture (460 μL) was quenched with 460 μL of 8.5% phosphoric acid and washed twice with 4 and 2 mL of ethyl acetate, respectively. The combined ethyl acetate portions were concentrated under reduced pressure, and the residue was dissolved in 1 mL of 40% acetonitrile/water. Purification of HPT-cys was conducted using the same HPLC conditions described above. The fraction containing HPT-cys was lyophilized and submitted for mass spectrometry analysis. LC-MS: HRMS calcd for $C_{13}H_{15}N_2O_4S_2$ 327.0473, found 327.0460. This mass measurement was made using a JEOL model SX102A mass spectrometer; measurements were made at 10 000 resolution (10% valley definition) (Mass Spectrometry Facility, Department of Chemistry and Chemical Biology, Harvard University).

To isolate a large quantity of HPT-cys in the $H_2{}^{18}O$ experiment, conditions were as above except that 1 mM salicylate, 5 mM ATP, and 2 μM HMWP2 1−1491 were used, and the ratio of $H_2{}^{18}O$ and $H_2{}^{16}O$ was adjusted to 49:51.

(c) Isolation of HPT-COOH for Mass Spectrometry Analysis. To prepare HPT-COOH for HPLC purification and mass spectrometry, the following were incubated at 37 °C for 5 h, 75 mM Tris-HCl, pH 8.8, 10 mM $MgCl_2$, 5 mM DTT, 1 mM CoASH, 10 mM ATP, 0.2 mM L-cysteine, 1 mM salicylate, 0.1 μM YbtE, 1 μM EntD, and 2 μM HMWP2 1−1491, to a final volume of 1 mL. The reaction was quenched with 200 μL of 8.5% phosphoric acid and washed twice with 5 mL of ethyl acetate. After concentration of the combined organic layers under reduced pressure, the residue was dissolved in 30% acetonitrile/water. Purification of HPT-COOH was conducted using the same HPLC conditions described above. LC-MS *m*/*z* (relative intensity): 224 ([M + H]$^+$, 100), 222 (85), 204 (27). LC-MS measurements were performed using a Micromass Platform II quadrupole mass spectrometer (Micromass, Beverly, MA) using an atmospheric pressure chemical ionization source (Mass Spectrometry Facility, Department of Chemistry and Chemical Biology, Harvard University).

Synthesis of Standard Compounds for the HMWP2 1−1491 Assay. ^{1}H NMR spectra were recorded using a 500 MHz Bruker AM-500 spectrometer (NuMega, California). Chemical shifts are given in ppm relative to tetramethylsilane (δ = 0 ppm). Low-resolution mass spectra were recorded using a JEOL model AX505H mass spectrometer (JEOL Ltd., Akishima, Japan). Accurate mass measurements were performed using a JEOL model SX102A mass spectrometer (Mass Spectrometry Facility, Department of Chemistry and Chemical Biology, Harvard University).

Salicyl-cysteine (*29*) and HPT-COOH (*30*) were prepared according to published procedures.

HPT-cys was prepared as described below. To a mixture of HPT-COOH (2.23 g, 10 mmol), cystine dimethyl ester dihydrochloride (1.71 g, 5 mmol) and benzotriazol-1-yl-oxytripyrrolidinophosphonium hexafluorophosphate (PyBop, 7.80 g, 15 mmol) in 100 mL of dichloromethane was added *N*,*N*′-diisopropylethylamine (3.6 mL, 20 mmol). The mixture

was stirred for 1 h at room temperature. The resulting yellowish solution was washed with 200 mL of water, dried over $MgSO_4$, and concentrated. The residue was dissolved in 100 mL of ethyl acetate, and crystallized material was removed by filtration. The filtrate was concentrated and dissolved in 100 mL of ethanol, and then 10 mL of 1 N ammonium hydroxide was added. A gel started to form after 5 min. DTT (3.0 g, 19.5 mmol) was added to the mixture, and the resulting solution was stirred for 2 h at room temperature. The solution was then diluted with 200 mL of water and extracted with ether (2 × 100 mL). The combined organic layers were washed with 50 mL of water, dried over $MgSO_4$, and concentrated. The crude product was purified by silica gel chromatography (100% dichloromethane then dichloromethane:ethyl acetate = 10:1) to give 2.49 g (73%) of HPT-cys methyl ester (a 3:7 mixture of diastereomers) as colorless crystals: mp 102−107 °C. ^{1}H NMR (DMSO-d_6) δ: 12.15 (s, 0.3 H), 12.13 (s, 0.6 H), 8.78 (d, 0.6 H, J = 7.8 Hz), 8.75 (d, 0.3 H, J = 8.0 Hz), 7.44 (m, 2), 6.99 (m, 3), 5.42 (t, 1 H, J = 8.8 Hz), 4.53 (m, 1), 3.67 (s, 0.9 H), 3.67 (m, 1 H), 3.66 (s, 2.1 H), 3.58 (m, 1 H), 2.93 (m, 1 H), 2.85 (m, 1H), 2.60 (t, 0.3 H, J = 8.7 Hz), 2.52 (t, 0.7 H, J = 8.5 Hz). FAB-MS m/z (rel intensity): 363 ($[M + Na]^+$, 67) 341 ($[M + H]^+$, 100), 340 (48), 203 (54).

A suspension of the above-prepared HPT-cys methyl ester (170 mg, 0.5 mmol) in a mixture of 10 mL of methanol and 1 mL of 1 N NaOH was stirred for 1.5 h at room temperature. The resulting solution was acidified to pH 2 with 85% phosphoric acid, concentrated to half the volume under reduced pressure, and diluted with 20 mL of water. The mixture was extracted with ethyl acetate, the organic layer was dried over $MgSO_4$, and this concentrated to give a quantitative yield of HPT-cys (1:1 mixture of diastereomers) as a yellowish solid: mp 128−133 °C. ^{1}H NMR (DMSO-d_6) δ: 12.72 (bs, 1 H), 12.15 (s, 1 H), 8.61 (d, 0.5 H, J = 7.5 Hz), 8.58 (d, 0.5 H, J = 8.1 Hz), 7.46 (m, 2 H), 6.97 (m, 2 H), 5.42 (t, 2 H, J = 10.1 Hz), 4.46 (m, 1 H), 3.69 (apparent t, 1 H, J = 10.6 Hz), 3.58 (apparent t, 1 H, J = 10.1 Hz), 2.94 (m, 1 H), 2.84 (m,1 H), 2.48 (t, 0.5 H, J = 10.1 Hz), 2.40 (t, 0.5 H, J = 13.5 Hz). HRMS m/z calcd for $C_{13}H_{15}N_2O_4S_2$: 327.0473. Found: 327.0480.

RESULTS

Domain Architecture of HMWP2 and Design of Enzyme Fragments. The *Y. enterocolitica irp2* gene encoding the 2035 aa HMWP2 was previously sequenced, and this protein was identified as a member of the nonribosomal peptide synthetase family on the basis of sequence similarity to other antibiotic and siderophore synthetases (*22*). Several domains of HMWP2 were noted including an amino acid adenylation domain, two serine phosphopantetheinylation domains centered around Ser52 and Ser1439, and two direct repeats of unknown function on either side of the adenylation domain. We have further investigated the domain structure of HMWP2 by sequence analysis and propose the seven-domain structure presented in Figure 1.

Modification of certain serine residues by covalent attachment of a Ppant cofactor is absolutely required for the activity of nonribosomal peptide synthetases, and these serine residues may be recognized by the canonical sequence surrounding them (reviewed in *31*). Guilvout et al. (*22*) noted

Scheme 2

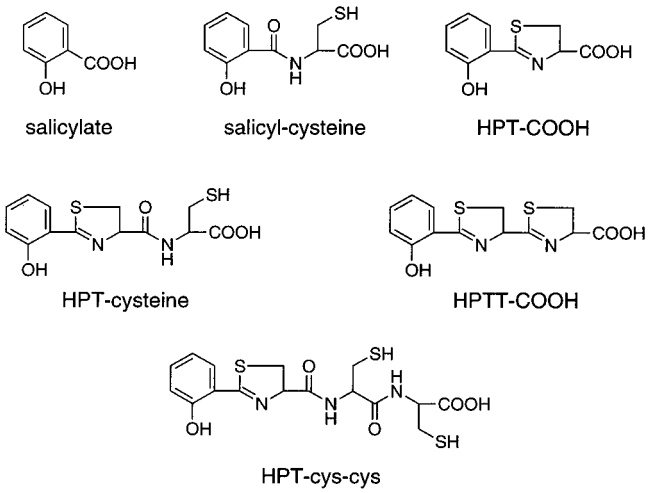

two potential phosphopantetheinylation sites in HMWP2, Ser52 and Ser1439, and we propose a third site at the C-terminal end of the protein, Ser1977. The local sequence environment of each serine phosphopantetheinylation site is noted in Figure 1. The first 100 N-terminal amino acids of HMWP2 are identified as an ArCP domain by similarity to *E. coli* EntB (*24*), while HMWP2 1383−1491 and HMWP2 1927−2035 are designated PCP1 and PCP2, respectively, on the basis of similarity to peptide synthetases.

Guilvout et al. (*22*) reported that the central amino acid adenylation domain of HMWP2 (residues 545−1382) is interrupted by an approximately 340 aa stretch (1011−1347) with no homology in the database. We have detected weak homology in this region to methyltransferases (*32*). On the basis of similarity to the recently sequenced bacitracin synthetase (*33*), the direct repeats found on either side of the HMWP2 adenylation domain (*22*) (residues 101−544, 1492−1926) can now be described as condensation/cyclization domains.

With an ArCP, two PCP domains, and two condensation/cyclization domains, HMWP2 is expected to covalently load 1 equiv of salicylate and 2 equiv of cysteine to form the hydroxyphenyl-thiazolinyl-thiazoline carboxylate (HPTT-COOH) portion of the final yersiniabactin molecule (Scheme 2). To investigate the functions of some of these HMWP2 domains, fragments of the *Y. pestis* enzyme were overproduced in *E. coli* and purified as described in Materials and Methods (Figure 2). To aid in purification, each HMWP2 fragment was expressed as a C-terminal hexahistidine tag fusion. The N-terminal ArCP domain (residues 1−100, 12.7 kDa) and the internal PCP1 domain (residues 1383−1491, 13.4 kDa) were reasonably soluble, and 30−40 mg of protein could be obtained per liter of *E. coli* culture (data not shown). The large HMWP2 fragment (residues 1−1491) containing the first five of seven domains of the full-length protein (ArCP, condensation/cyclization, adenylation, methyltransferase, PCP) was only sparingly soluble, even when *E. coli* cultures were grown at room temperature, and did not bind well to the nickel affinity column (data not shown). However, in the best case, about 3 mg of HMWP2 1−1491 could be obtained per liter of *E. coli* culture.

YbtE is a Salicyl-AMP Ligase Capable of the Covalent Acylation of the ArCP Domain of HMWP2. On the basis of

Table 1: Kinetic Parameters for the ATP−PP_i Exchange Reactions Catalyzed by YbtE and HMWP2 1-1491

substrate	k_{cat} (min^{-1})	K_m (μM)	k_{cat}/K_m (μM^{-1} min^{-1})
YbtE Reactions			
ATP	270	350	0.77
Salicylate	230	4.6	50
DHB	14	400	0.035
HMWP2 1-1491 Reactions			
ATP	500	360	1.4
L-Cysteine	380	650	0.58

the 61% similarity of *Y. pestis* YbtE (*20*) to the *E. coli* enterobactin synthetase enzyme EntE (*24*), we expected YbtE to catalyze the adenylation of salicylate and the transfer of the salicyl group to the HMWP2 ArCP (Figure 1). The *Y. pestis* YbtE was overproduced in *E. coli* as an N-terminal histidine tag fusion protein and purified by nickel chelate chromatography with a yield of 60 mg per liter of *E. coli* culture (data not shown). The purified YbtE had robust salicylate-dependent catalytic activity in the radioactive isotope exchange ATP-$^{32}PP_i$ assay, the characteristic assay for measurement of the reversible formation of acyl-AMP, in this case salicyl-AMP. The salicylate adenylation reaction proceeded with an average k_{cat} of 250 min^{-1}, a K_m for salicylate of 4.6 μM, and a K_m for ATP of 350 μM (Table 1). YbtE could also catalyze the adenylation of DHB, the cognate substrate of EntE, albeit with a 1400-fold lower catalytic efficiency as compared to the salicylate adenylation reaction (Table 1).

To assess whether YbtE could use salicyl-AMP as an acyl donor to the N-terminal domain of HMWP2, the HMWP2 ArCP fragment was used as a substrate (Figure 2). In order for salicylate to be covalently attached to this ArCP fragment, it must be in the postranslationally modified, phosphopantetheinylated holo-form. Holo-HMWP2 ArCP was formed by reaction of the apo-ArCP (as purified from *E. coli* lysates) with CoASH and the *E. coli* phosphopantetheinyl transferase (PPTase) enzyme EntD which modifies the enterobactin synthetase (*24*, *28*). EntD could catalyze phosphopantetheinylation of the apo-HMWP2 ArCP with a k_{cat} of 1.5 min^{-1} and K_m for the ArCP fragment of 9.9 μM (Figure 3A); this compares favorably to a k_{cat} of 7 min^{-1} and a K_m of 8 μM for EntD and its cognate substrate, the apo-ArCP domain of EntB (*24*). The EntD-dependent phosphopantetheinylation of the apo-HMWP2 ArCP was visualized by autoradiography as the covalent incorporation of radioactivity from [^{3}H]-CoASH (Figure 4, lane 2).

With holo-HMWP2 ArCP in hand, the ability of YbtE to transfer [^{14}C]salicylate to this HMWP2 fragment could be assessed. As judged by TCA precipitation of radioactivity from [^{14}C]salicylate into the protein pellet, YbtE could efficiently load the holo-HMWP2 ArCP with salicylate. This reaction proceeded with a k_{cat} of 94 min^{-1} and K_m for the ArCP acceptor substrate of 5.6 μM (Figure 3B). The covalent nature of the salicylation of the holo-ArCP fragment was further established by autoradiography of the 12.7 kDa fragment after SDS−PAGE (Figure 5, lane 2). The much larger (168 kDa) holo-HMWP2 1−1491 was also well-labeled with [^{14}C]salicylate in a YbtE-dependent manner, presumably at the N-terminal ArCP site (Figure 5, lanes 6 and 7). YbtE did not transfer [^{14}C]salicyl radioactivity to holo-PCP1 (Figure 5, lane 4) under the same conditions

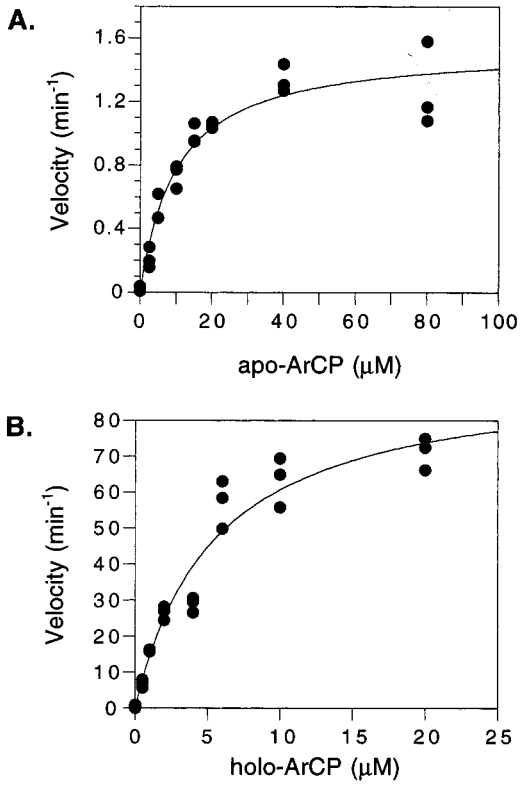

FIGURE 3: (A) Velocity versus substrate concentration plot for the phosphopantetheinylation of the HMWP2 ArCP by *E. coli* EntD. EntD (25 nM) was incubated for 15 min with [^{3}H]CoASH (150 μM, 200 Ci/mol) and increasing concentrations of the apo-ArCP fragment. From this curve, a k_{cat} of 1.5 min^{-1} and a K_m value for the ArCP substrate of 9.9 μM are calculated. (B) Velocity versus substrate concentration plot for the acylation of the HMWP2 holo-ArCP fragment with [^{14}C]salicylate catalyzed by YbtE. YbtE (2.5 nM) was incubated for 5 min with [^{14}C]salicylate (90 μM, 55.5 Ci/mol), ATP (5 mM) and increasing concentrations of the holo-ArCP fragment. From this curve, a k_{cat} of 94 min^{-1} and a K_m value of 5.6 μM for the holo-ArCP substrate are calculated.

where ArCP is clearly labeled, indicating that YbtE can discriminate between the phosphopantetheinylated forms of ArCP and PCP domains. YbtE showed no detectable salicyl transfer to the holo-ArCP domain of EntB, validating a specific recognition of YbtE for the protein scaffolding of the N-terminal ArCP domain of HMWP2; EntE was able to recognize the holo-HMWP2 ArCP, but with a greatly elevated K_m for the protein substrate (data not shown).

Catalytic Properties of the Five Domain Fragment HMWP2 1−1491

(A) Peptidyl Carrier Protein Domains. In addition to the N-terminal ArCP domain, HMWP2 1−1491 has a C-terminal PCP domain, with a potential phosphopantetheinylation site at Ser1439. Apo-PCP1 could be phosphopantetheinylated by the PPTases (*28*) *E. coli* EntD or *B. subtilis* Sfp. As shown in Figure 4 (lane 4), incubations of apo-PCP1, EntD, and [^{3}H]CoASH led to covalent tritiation of the 13.4 kDa PCP1. Tritiation of HMWP2 1−1491, which contains the ArCP and PCP1 domains, is also confirmed in Figure 4 (lane 6). Holo-PCP1 was prepared and then used as a potential substrate for cysteinylation by the HMWP2 1−1491 enzyme (see below). The second PCP domain of HMWP2, centered around Ser1977, was also overproduced in *E. coli*, purified, and tested as a substrate for EntD. PCP2 (residues 1927−

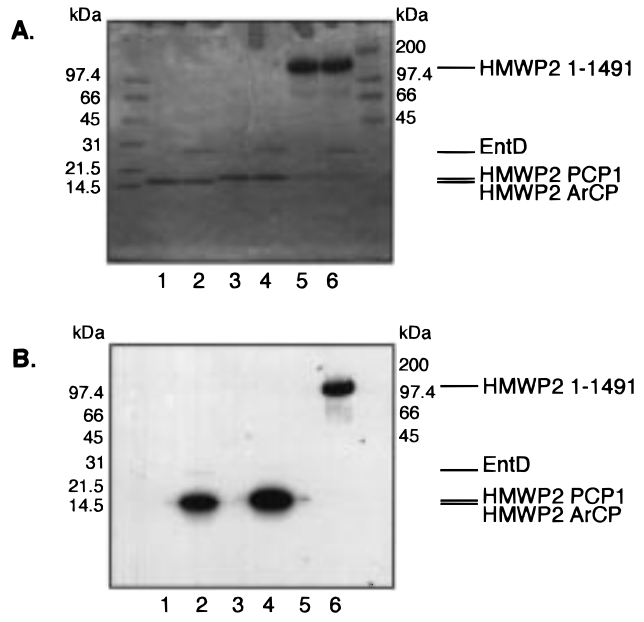

FIGURE 4: Demonstration of the phosphopantetheinylation of the apo-HMWP2 ArCP, PCP1, and 1−1491 fragments dependent on *E. coli* EntD. (A) Coomassie-stained gel (4−20%) of TCA-precipitated reaction mixtures. (B) Autoradiograph of this gel. All reaction mixtures contained [^{3}H]CoASH (150 μM, 192 Ci/mol) and where indicated EntD (800 nM). Lane 1, HMWP2 ArCP (6 μM); lane 2, HMWP2 ArCP with EntD; lane 3, HMWP2 PCP1 (6 μM); lane 4, HMWP2 PCP1 with EntD; lane 5, HMWP2 1−1491 (1 μM); lane 6, HMWP2 1−1491 with EntD.

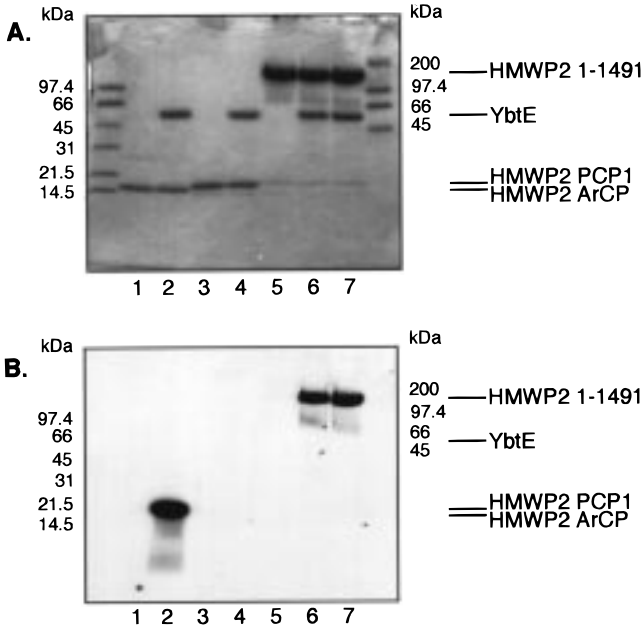

FIGURE 5: Demonstration of the acylation of the HMWP2 ArCP and 1−1491 fragment with [^{14}C]salicylate dependent on YbtE. (A) Coomassie-stained gel (4−20%) of TCA-precipitated reaction mixtures. (B) Autoradiograph of this gel. All reaction mixtures contained [^{14}C]salicylate (90 μM, 55.5 Ci/mol) and ATP (10 mM) and where indicated YbtE (1 μM). Lane 1, holo-ArCP (6 μM); lane 2, holo-ArCP with YbtE; lane 3, holo-PCP1 (6 μM); lane 4, holo-PCP1 with YbtE; lane 5, holo-HMWP2 1−1491 (1 μM); lane 6, holo-HMWP2 1−1491 with YbtE; lane 7, holo-HMWP2 1−1491 with YbtE and cysteine (3 mM).

2035) was successfully phosphopantetheinylated, validating the designation of this domain as a PCP (data not shown).

(B) Cysteine-AMP Formation and Transfer to PCP1. On the basis of the structure of yersiniabactin, it was expected

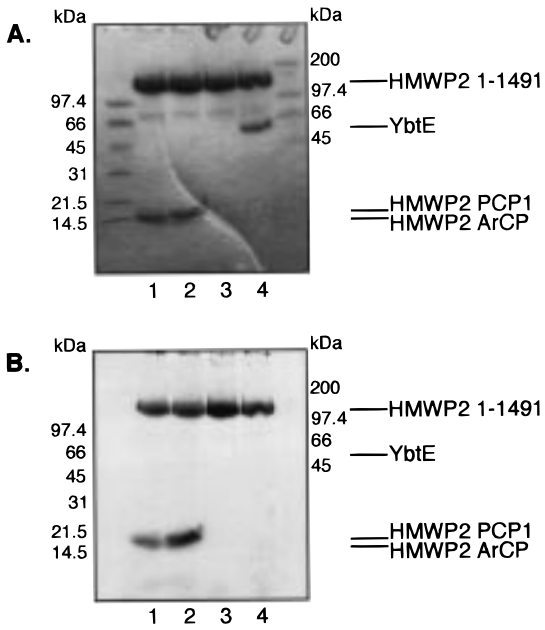

FIGURE 6: Demonstration of the covalent loading of the HMWP2 fragments with [^{35}S]-L-cysteine. (A) Coomassie-stained gel (4−20%) of TCA-precipitated reaction mixtures. (B) Autoradiograph of this gel. All reaction mixtures contained [^{35}S]cysteine (0.68 mM, 55.5 Ci/mol) and ATP (10 mM). Lane 1, holo-ArCP (15 μM) and apo-HMWP2 1−1491 (1 μM); lane 2, holo-PCP1 (15 μM) and apo-HMWP2 1−1491 (1 μM); lane 3, holo-HMWP2 1−1491 (1 μM); lane 4, holo-HMWP2 1−1491 (1 μM) with salicylate (1 mM) and YbtE (1 μM). In the absence of ATP, no [^{35}S]-labeling of any of these proteins is observed (data not shown).

that the central HMWP2 1−1491 adenylation domain would catalyze the adenylation of L-cysteine. Indeed, pure HMWP2 1−1491 displayed cysteine-dependent ATP-^{32}PP$_i$ exchange with an average k_{cat} of 440 min^{-1} and K_m values of 650 μM and 360 μM respectively for the L-cysteine and ATP substrates (Table 1). No ATP-^{32}PP$_i$ exchange was observed when serine was used as the amino acid substrate (data not shown). A HMWP2 1−1061 fragment was also purified which failed to support ATP-^{32}PP$_i$ exchange, confirming that the A9 and A10 core domains of the adenylation domain (*31*) which follow the putative methyltransferase domain are absolutely required for adenylation activity (data not shown). Methyltransferase activity of the interrupting domain has not yet been assessed.

Following the demonstration of cysteine-adenylating activity by HMWP2 1−1491, the ability of this enzyme to transfer the activated cysteine group to its own integrated PCP domain or intermolecularly to the isolated PCP1 fragment was assessed. HMWP2 1−1491 was incubated with [^{35}S]-L-cysteine and ATP, and the reaction mixtures were subjected to SDS−PAGE and autoradiography (Figure 6). HMWP2 was capable of self-aminoacylation with cysteine (lanes 3 and 4) as well as intermolecular transfer of cysteine to the PCP1 fragment (lane 2). The ATP-dependence of this [^{35}S]-cysteine labeling was verified by scintillation counting of TCA-precipitated reaction mixtures and autoradiography (data not shown). In Figure 6, lanes 1 and 2, it should be noted that apo-HMWP2 1−1491 is clearly labeled with [^{35}S]-cysteine. ATP-dependent labeling of the apo-HMWP2 1−1491 preparation with [^{35}S]cysteine was verified by scintillation counting of TCA-precipitated reaction mixtures (4% labeling); under similar reaction conditions, the holo-

HMWP2 1−1491 preparation acquires 6-fold more radioactivity (22% labeling) (data not shown). This labeling of the apo-HMWP2 1−1491 preparation with [^{35}S]cysteine may either indicate the partial in vivo phosphopantetheinylation of HMWP2 1−1491 when overproduced in *E. coli* or possibly adventitious reaction of the cysteinyl-AMP with groups other than the Ppant cofactor (reaction of aminoacyl-adenylates and the formation of a covalent adduct with the producing aminoacyl-tRNA synthetase enzyme has been observed in some cases (*34*)). Loading of PCP1 (and ArCP) with [^{35}S]cysteine by HMWP2 1−1491 does require the phosphopantetheinylation of the carrier protein substrate (data not shown). While the signal is weak, HMWP2 1−1491 is also capable of aminoacylating the HMWP2 ArCP domain fragment with [^{35}S]cysteine (Figure 6, lane 1). YbtE seems to be better able to discriminate between isolated ArCP and PCP domains than the HMWP2 1−1491 fragment.

These results provide functions for the ArCP domain, the adenylation domain, and the PCP1 domain of HMWP2 and leave the role of the condensation/cyclization domain, residues 101 to 544, to be addressed.

(C) Release of Cyclized Product from HMWP2 1−1491. In analogy to the enterobactin synthetase case (Figure 1) where the mixing of DHB, serine, and ATP substrates with EntE, EntB, and EntF led to EntF-catalyzed amide bond formation and generation of the aryl-N-ser-S-PCP covalent acyl enzyme intermediate (*25*), it was anticipated that YbtE and HMWP2 1−1491, in the presence of salicylate, ATP, and cysteine, should yield either salicyl-cys-S-PCP1 or the cyclized thiazoline variant, the hydroxyphenylthiazolinyl-carbonyl-S-PCP1 form of HMWP2 in up to stoichiometric quantities. We had achieved some success in base-catalyzed hydrolysis of the DHB-ser-S-EntF intermediate at pH 8.8, leading to release of the aryl-N-capped serine into solution for detection by thin-layer chromatography (*25*). We conducted incubations of YbtE and holo-HMWP2 1−1491 (by preincubation with CoASH and EntD) with salicylate, cysteine, and ATP at pH 8.8 and analyzed the solution over time by HPLC for any products released. As shown in Scheme 2, various standards including salicylate, salicyl-cysteine, HPT-COOH [also known as the natural product dihydroaeruginoate (*35*)], HPT-cysteine, and the bisthiazoline HPTT-COOH were considered as potential products.

The HPLC traces in Figure 7A show formation of a prominent peak, detectable within 5 min, in incubations containing 2 μM HMWP2 1−1491 that forms in amounts much greater than stoichiometric. The amount of this product formed over the 2 h time period is cleanly linear (Figure 7B). Synthesis of this product is absolutely dependent on the presence of YbtE, the 170 kDa HMWP2 1−1491 fragment, cysteine, and salicylate in the reaction mixture (Figure 7C). By HPLC co-injection with the standards of Scheme 2, the enzymatic product appeared to be HPT-cysteine. The peak containing the putative HPT-cys was purified and submitted for high-resolution mass spectrometry analysis; a mass of 327 was determined for the reaction product, in perfect agreement with the calculated mass of protonated HPT-cys as well as the mass of the protonated HPT-cys standard compound (Table 2). From the integrated area of the HPLC traces graphed in Figure 7B, the k_{obs} for HPT-cys release from HMWP2 1−1491 under the indicated conditions is 1 min^{-1}. Thus, up to 120 catalytic turnovers were observed during the linear 2 h time course. Minor amounts of a product with a mass of 430 were observed in Figure 7A (Table 2), consistent with its identification as M + H of HPT-cys-cys (Scheme 2), but this product was not pursued further.

These results were initially surprising in at least two respects, the large number of turnovers observed and the release of HPT-cys instead of HPT-COOH as the principal product. The enzymatic incubations analyzed in Figure 7A contained 5 mM DTT as well as 5 mM L-cysteine. When the DTT concentration was lowered to 0.5 mM, the reaction rate did drop, but there was no change in the composition of released product (data not shown). However, when the cysteine concentration was lowered to 0.2 mM (Figure 7D), while HPT-cys formation was still robust, now a bit more than half of the product migrated as HPT-COOH. This identification was validated both by co-injection on HPLC with the authentic standard and by mass spectrometry where the expected mass of 224 was observed (Table 2). To evaluate whether the HPT-cys product arose from capture of HPT-S-enzyme by cysteinyl-AMP stalled in the adenylation domain active site of HMWP2 1−1491, incubations were conducted with 5 mM cysteine in 50% $H_2{}^{18}O$ to look for any M + 2H product (mass of 328) that would arise by release of HPT-cys-AMP and then hydrolysis of the mixed anhydride in heavy water. Only a mass of 327 was detected corresponding to the $[M + H]^+$ ion of HPT-cys, arguing strongly for transthiolation and release of HPT-S-enzyme by cysteine either free in solution or bound to the enzyme but not adenylated.

DISCUSSION

The studies reported here provide the first enzyme-based information on the function of *Y. pestis* YbtE and HMWP2 and establish the role of these proteins in the biosynthesis of the yersiniae siderophore, yersiniabactin. YbtE and HMWP2 (residues 1−1491) are responsible for the initiation and elongation of the left-hand portion of the yersiniabactin molecule, the hydroxyphenylthiazoline moiety. The *ybtE* and *irp2* genes (*20, 23*) encoding these yersiniabactin synthetase enzymes have been localized to a high pathogenicity island on the chromosome of pathogenic *Yersinia* species (*Y. pestis*, *Y. enterocolitica*, *Y. pseudotuberculosis*) (*14*−*17*). Numerous studies have correlated the presence of this cluster of iron regulated genes, particularly *irp2*, to the virulence of *Yersinia* species (*1, 20, 36*−*42*). The production of siderophores has also been correlated with the virulence of *Yersinia* species (*5, 7, 43*), and we demonstrate conclusively here the biochemical role of YbtE and HMWP2 in the biogenesis of the yersiniabactin siderophore.

Given the documented relationship of the yersiniabactin synthetase enzymes to yersiniae virulence, these siderophore-synthesizing enzymes may represent unexploited targets for interventional strategies to render *Yersinia* avirulent. The devastating disease plague, caused by *Y. pestis*, is considered a reemerging disease with increased numbers of cases reported around the world (*18, 44*). Even more frightening, a multidrug resistant strain of *Y. pestis* bearing a highly transferable multidrug-resistance plasmid was recently isolated (*44*). *Y. pestis* may not remain universally susceptible to traditional antibiotic treatment, encouraging the development

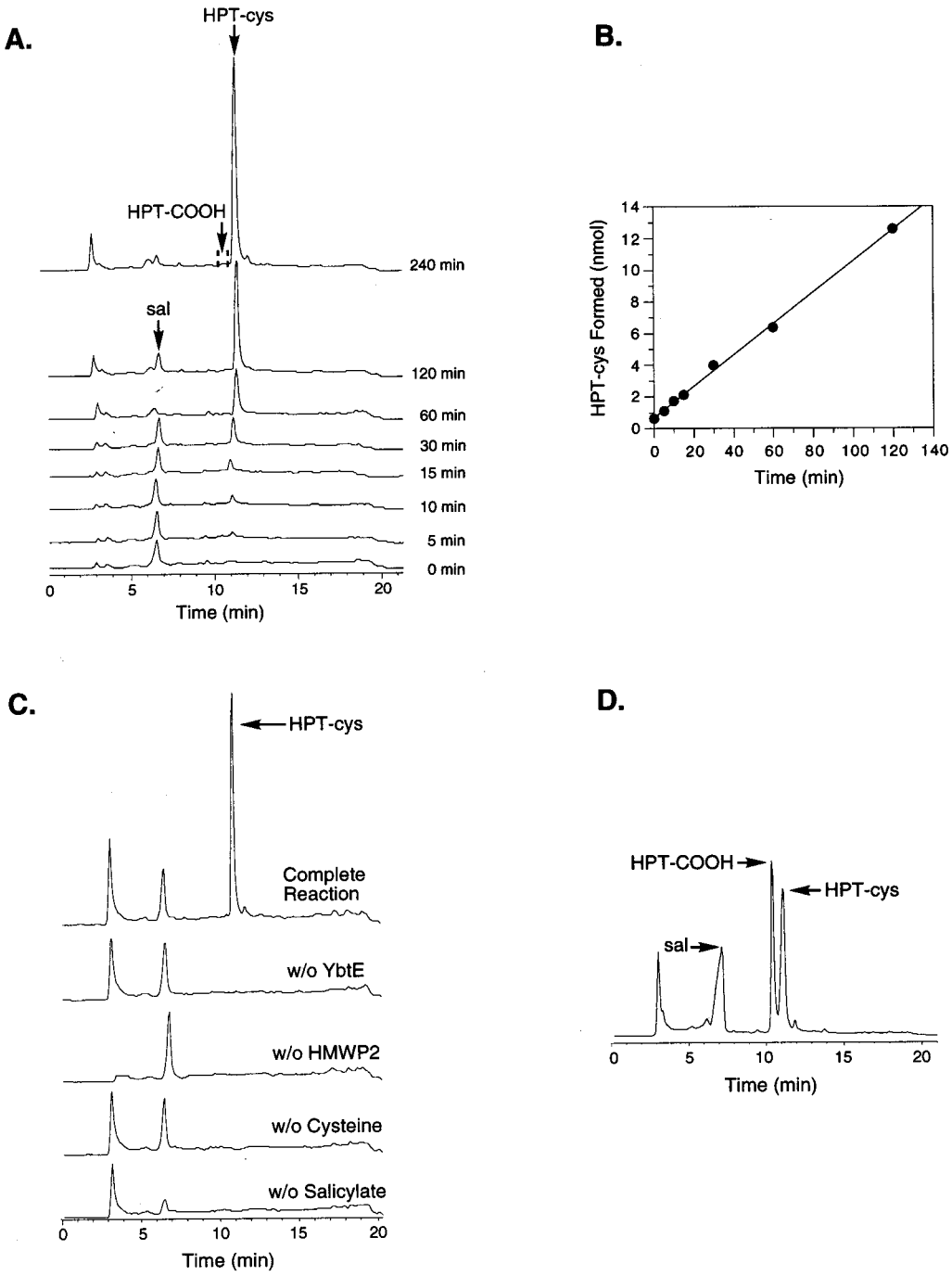

FIGURE 7: (A) HPLC traces of a time course of HPT-cys formation by YbtE and HMWP2 1−1491 in the presence of the substrates cysteine (5 mM), salicylate (1 mM) and ATP (10 mM). The major peak at 11.68 min was identified as HPT-cys by both co-injection with a synthetic standard and high-resolution mass spectrometry. Minor peaks at 6.99 and 12.40 min represent salicylate and HPT-cys-cys, respectively, as determined by co-injection and mass spectral analysis, respectively. (B) Plot showing the linearity of the time course of HPT-cys formation shown in A. From this line, a k_{obs} of 1 min^{-1} for HPT-cys formation is calculated. (C) HPLC traces demonstrating the requirement of YbtE, HMWP2 1−1491, cysteine, and salicylate for HPT-cys formation. (D) HPLC trace of the reaction of YbtE and HMWP2 1−1491 at low cysteine concentration (0.2 mM) (5 h incubation). Under these conditions, the amount of HPT-COOH formed ($k_{obs} \approx 0.035$ min^{-1}) is comparable to the amount of HPT-cys.

of new methods for its control. The molecular machinery responsible for synthesizing other siderophores such as vibriobactin and pyochelin (Scheme 1) will likely resemble the yersiniabactin synthetase, so antibiotics which target the yersiniabactin synthetase may also be effective against the siderophore-synthesizing systems of other pathogenic bacterial species.

The detection of the unusual heterocyclization capacity of HMWP2 1−1491 provides the first opportunity to characterize this type of reaction in a nonribosomal peptide synthetase enzyme. Not only are heterocyclic ring structures of the thiazole/oxazole group found in other siderophore molecules (Scheme 1) but they are also found in a broadly interesting therapeutic class of natural products. These include the antitumor drugs bleomycin (*45*) and epothilone (*46*), the protein synthesis inhibitor antibiotics thiostrepton (*47*) and GE2270A (*48*), the bacterial cell-wall-directed topical antibiotic bacitracin A (*49*), and the DNA gyrase

Table 2: Mass Spectral Data ($[M + H]^+$ Values) Obtained for Standard Compounds and the HPLC-Purified Products of the HMWP2 1-1491 Reaction

compound	calcd mass (Da)	obs mass of standard compound (Da)	obs mass of HMWP2 product (Da)
salicyl-cysteine	242	(240 for $[M - H]^-$)	
HPT-COOH	224	224	224
HPT-cysteine	327.0473	327.0480	327.0460
HPT-cys-cys	430		430

inhibitor microcin B17 (*50*). The first efforts at deconvoluting an enzymatic strategy of peptide heterocyclization have recently been reported for the microcin B17 synthetase system (*51*). Residues of the *E. coli* peptide antibiotic microcin A are posttranslationally converted to the four thiazole and four oxazole rings in the mature antibiotic microcin B17 catalyzed by the three subunit microcin synthetase modifying enzyme. Postranslational heterocyclization as exemplified by the microcin synthetase represents one paradigm for the enzymatic generation of heterocyclic ring structures. The successful purification of an active, thiazoline-ring-forming HMWP2 enzyme fragment allows exploration of a second paradigm for heterocycle formation—cyclodehydration occurring during peptide chain assembly while the growing chain is covalently tethered to the phosphopantetheine cofactor of a PCP domain in a multimodular peptide synthetase. The strategy elucidated for yersiniabactin synthesis should have application to the synthesis of other thiazole-/oxazole-containing nonribosomal peptide antibiotics such as bacitracin A, bleomycin, and GE2270A.

Building from an organizational homology of YbtE and HMWP2 to the recently deciphered enterobactin synthetase (*24*, *25*) (Figure 1) and the comparable aryl N-capped peptides which should be produced by these enzymes (2,3-dihydroxybenzoyl-ser versus 2-hydroxybenzoyl-cys), we have proven several functions for YbtE and HMWP2 that validate the architectural and chemical relatedness of the biosynthetic strategies for enterobactin and yersiniabactin siderophore biogenesis. First, we have demonstrated that YbtE is a salicyl-AMP ligase that specifically loads the N-terminal ArCP domain of HMWP2 with salicylate in thioester linkage to its Ppant prosthetic group (presumably at Ser52). This is analogous to the activity of EntE which adenylates DHB (or salicylate) and then transfers the dihydroxybenzoyl group to the holo-ArCP domain of EntB (*24*). As in enterobactin biosynthesis, loading of an ArCP domain (HMWP2) with an hydroxybenzoyl group (salicylate) catalyzed by an AMP-ligase (YbtE) is the initiating step in siderophore chain growth. YbtE shows two kinds of specificity which indicate that protein—protein recognition accompanies this enzyme's scan for a phosphopantetheinyl tether thiol terminus prior to donation of the acyl group from salicyl-AMP. YbtE will neither catalyze salicyl transfer to the corresponding holo-form of the ArCP domain of EntB nor detectably salicylate the holo-form of the PCP1 domain expressed as a 13 kDa fragment from residues 1383—1491 of HMWP2.

HMWP2 also demonstrates considerable organizational and functional homology to *E. coli* EntF, the catalyst for enterobactin elongation by amide and ester bond formation. The adenylation domain of HMWP2 (residues 545—1382), assayed using the HMWP2 1—1491 enzyme fragment, catalyzes the adenylation of cysteine with an efficiency comparable to that for the adenylation of serine by EntF (*52*) and is capable of self-aminoacylation, presumably on the holo-PCP1 domain as demonstrated by autoradiography to give a Cys-S-Ppant-PCP1-HMWP2 intermediate. The comparable Ser-S-Ppant-PCP-EntF intermediate has been indicated in enterobactin biosynthesis (*25*). The HMWP2 1—1491 fragment was further shown to carry out this aminoacylation reaction "in trans", labeling the purified holo-PCP1 domain (residues 1383—1491) with [^{35}S]cysteine. Weak "in trans" labeling of the holo-HMWP2 ArCP domain indicates the relaxed specificity of this intermolecular aminoacylation reaction as opposed to the very specific acylation reaction catalyzed by the naturally "in trans" YbtE/HMWP2 ArCP system. It should be noted that these experiments are made possible by the relaxed specificity of the *E. coli* PPTase EntD, which is capable of phosphopantetheinylating and thus making active the *Y. pestis* carrier protein domains; the comparable *Y. pestis* PPTase has so far not been discovered.

HMWP2 is a complex and intriguing combination of scaffold and catalyst, and while much of its catalytic activity can be predicted on the basis of domain homology to the enterobactin synthetase, this enzyme offers several unique features. One can discern in its 2035 length seven domains by homology to elements found in other nonribosomal peptide and/or siderophore synthetases (Figure 1). These include three phosphopantetheinylation sites distributed in an N-terminal ArCP (Ser52), an internal PCP (Ser1439), and a C-terminal PCP (Ser1977) domain. On the basis of the structure of yersiniabactin, both PCP domains are presumably loaded with cysteine prior to elongation and thiazoline/thiazolidine formation. However, there is only one adenylation domain located between residues 545—1382 in the HMWP2 sequence. In typical nonribosomal peptide synthetase organization, each PCP domain is preceded by an adenylation domain which loads its Ppant cofactor with the aminoacyl group (*31*). We propose that in the case of yersiniabactin biosynthesis, the one cysteine adenylation domain of HMWP2 loads cysteine onto both PCP1 (as demonstrated here) and PCP2 as well as a third PCP domain located in HMWP1 (A. M. G., I. M., C. T. W., R. D. P., unpublished observation). Although not discussed further here, we have been able to demonstrate cysteinylation of holo-PCP2 catalyzed by HMWP2 1—1491 (A. M. G., I. M., C. T. W., unpublished observation). To our knowledge, a situation in which one adenylation domain loads multiple PCP domains in cis and in trans is unique to the yersiniabactin synthetase.

The single adenylation domain of HMWP2 is also unusual when compared to other bacterial peptide synthetases in that it is interrupted between core motifs A8 and A9 (*31*) by a 340 amino acid insert showing similarity to methyltransferases. Methyltransferase consensus sequence motifs (*32*), particularly motif I (residues 1181—1189), can all be found in this HMWP2 domain. The fungal enniatin (*53*, *54*) and cyclosporin (*55*) synthetases have a similar interruption between motifs A8 and A9 of some adenylation domains by an *N*-methyltransferase domain. The fungal *N*-methyltransferase domains are about 100 aa longer than the HMWP2 insert, but do show homology to this insert in the

putative S-adenosylmethionine binding site (motif I). An X-ray crystal structure of the phenylalanine adenylation domain of the gramicidin synthetase was recently solved (*56*) and shows that the protein is folded into two interacting, compact subdomains: a large N-terminal lobe and a small C-terminal lobe. The adenylation core motifs (*31*) A1−A7 are found on the large lobe while A8−A10 are part of the small lobe; the putative methyltransferase insert of HMWP2 could be accommodated in this structure. In this study, we did not assess the functionality of this putative HMWP2 methyltransferase domain. The yersiniabactin structure shows the presence of three methyl groups in the right-hand portion of the molecule, and two putative methyltransferase domains have been noted in HMWP1 (A. M. G., I. M., C. T. W., unpublished observation).

The two repeated domains (residues 101−544, 1492−1926) in HMWP2 bear homology to condensation domains believed to be required for peptide bond formation in the nonribosomal peptide synthetases, but as discussed below actually conform most closely, with 44 and 51% homology, respectively, to the first condensation domain in the BA1 subunit of the bacitracin synthetase that has been postulated to be the site of thiazoline ring formation between Ile1 and Cys2 in that growing antibiotic chain (*33*). The studies reported here using the 170 kDa fragment of *Y. pestis* HMWP2 (1−1491) provide the first experimental evidence for the function of this domain in heterocycle formation.

Using the HMWP2 1−1491 enzyme fragment, containing this putative heterocyclization domain as well as an ArCP and a PCP domain, we expected to form stoichiometric amounts of a hydroxyphenylthiazolinylcarbonyl-S-Ppant-PCP1-HMWP2 intermediate upon incubation with YbtE, salicylate, cysteine, and ATP (Figure 8). To observe this intermediate, we tried mild base hydrolysis as a means of breaking the acyl−thioester linkage and cleaving this intermediate from the enzyme to facilitate its identification by HPLC and mass spectrometry. The gratifying but initially surprising result was that *catalytic* amounts of either the heterocyclized HPT-COOH or HPT-cysteine, depending on the cysteine concentration used in the assay, were produced in a YbtE- and HMWP2-dependent manner. The observation that both HPT-COOH and HPT-cys are released from HMWP2 indicates that either H_2O or cysteine can serve as the nucleophile for cleavage of the presumed hydroxyphenylthiazoline-thioester intermediate from the PCP1 domain of HMWP2 (Figure 8). The preponderant capture of the intermediate by cysteine when its concentration in the assay is high could be due to competition between direct aminolysis versus hydrolysis, or it could reflect initial thiolysis to an HPT-S-cysteine in solution which then undergoes acyl-S to -N shift. The cysteine nucleophile does not come from cysteinyl-AMP as indicated by incubations carried out in $H_2{}^{18}O$. The uncyclized salicyl-cysteine intermediate was not observed, demonstrating the efficiency of the cyclodehydration reaction under the conditions used. The k_{obs} of 1 min^{-1} for HPT-cys formation corresponds to hundreds of turnovers over the time period examined and sets a lower limit to the rate of enzyme-mediated condensation/heterocyclization. The stability of salicyl-cysteine has been examined, and at neutral pH there is no detectable thiazoline formation; conversely, HPT-COOH is stable for at least 3 days at neutral pH and has a half-life of 32 h at pH 2.5 (*29*). Thus, it is likely that

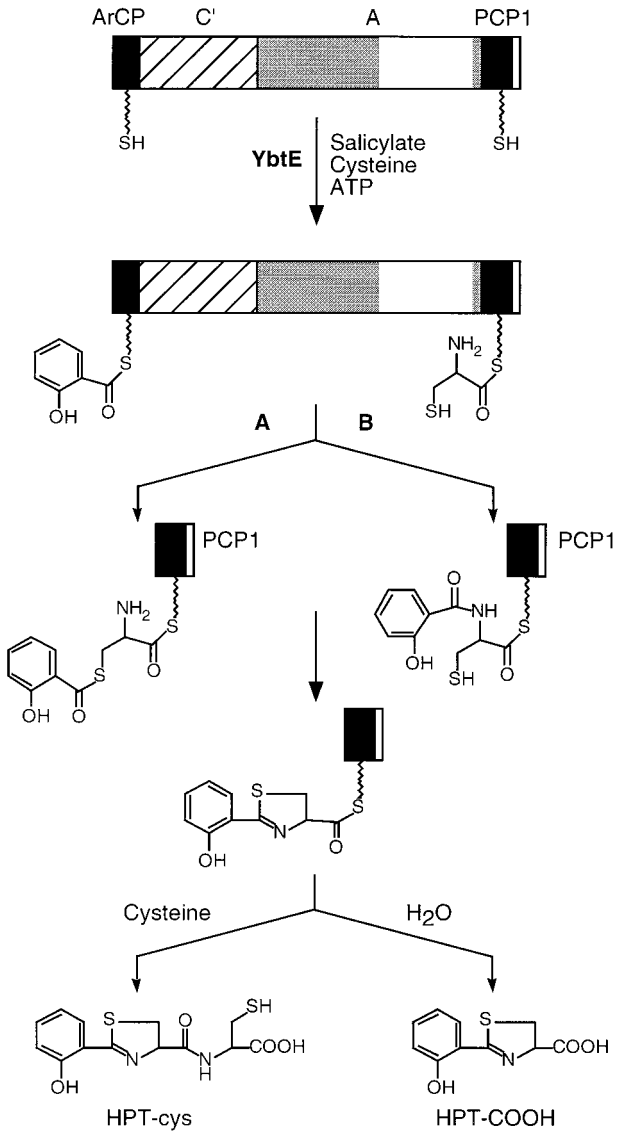

FIGURE 8: Proposed mechanism for the formation of HPT-COOH and HPT-cys catalyzed by HMWP2 1−1491. The holo-HMWP2 1−1491 fragment is covalently acylated with salicylate by YbtE on the ArCP domain and autoaminoacylated with cysteine on the PCP1 domain. The cysteine residue may attack the thioester linkage of the salicyl-Ppant-ArCP species using either its thio (pathway A) or amino (pathway B) groups as nucleophiles. In either case, heterocyclization gives the HPT-Ppant-PCP1 covalent species. Product may be released either by hydrolysis of the thioester linkage with water to give HPT-COOH or by nucleophilic attack of free cysteine giving the HPT-cys species.

the cyclization effected by the HMWP2 fragment is indeed enzyme-catalyzed and a special property of the unusual condensation/cyclization domain.

As described in Figure 8, the hydroxyphenylthiazoline intermediate could be formed through either a thioester or amide-bond linked intermediate by the attack of Cys-S-PCP1 onto salicyl-S-ArCP. Although the amide-bond formation route (pathway B of Figure 8) with the amino group of cysteine serving as the nucleophile is what one would expect based on the typical condensation domain precedent (*31*), the alternate route by pathway A, with the cysteine side chain thiolate anion as the attacking nucleophile also merits consideration. This pathway would not yield the amide salicyl-cysteine-S-PCP1-enzyme as intermediate but rather the acyl thioester salicyl-S-cys-S-PCP1-enzyme (a tandem

Table 3: Comparison of Core Motif 3 of Condensation Domains with the Same Region in the Putative Condensation/Heterocyclization Domains of Thiazoline/Oxazoline Ring-Forming Synthetases

enzyme	organism	position (aa)	sequence
	Domains Catalyzing Amide-Bond Formation[a]		
EntF	*Escherichia coli*	135	RY**HH**LLV**DG**F**S**FPAI
PvdD	*Pseudomonas aeruginosa*	171	VQ**HH**IVS**DG**W**S**MQVM
SnbC	*Streptomyces pristinaespiralis*	139	HV**HH**LLL**DG**YGFRLV
SrfA-A	*Bacillus subtilis*	1184	DM**HH**LIS**DG**V**S**IGIM
BA1 (BacA)	*Bacillus licheniformis*	1803	NF**HH**IIS**DG**V**S**QGIL
	Domains Catalyzing Bond Formation/Heterocyclization[b]		
HMWP2	*Yersinia pestis/enterocolitica*	244	NF**HH**IIS**DG**V**S**QGIL
HMWP2	*Yersinia pestis/enterocolitica*	1618	CL**D**NLLL**DG**L**S**MQIL
HMWP1[c]	*Yersinia pestis/enterocolitica*	2047	CL**D**NLLL**DG**L**S**MQIL
BA1	*Bacillus licheniformis*	764	NL**D**LLQF**D**VQ**S**FKVM
AngR	*Vibrio anguillarum*	140	RFNSVVV**D**NP**S**VILF
MTCY22H8.02	*Mycobacterium tuberculosis*	228	DL**D**MQAA**D**AM**S**YRIL

[a] All sequences available in the GenBank, SwissProt, or EMBL databases. [b] *Y. pestis* sequences obtained from R. D. Perry (unpublished). All other sequences available in the GenBank, SwissProt, or EMBL databases. [c] Amino acid 2045 for the *Y. enterocolitica* sequence.

thioester pair) by a transthiolation reaction. Heterocyclization from pathway A would then be the first half of an acyl-S to -N shift, with dehydration of the thiohemiaminal to yield the thiazoline *without ever forming the amide*. The 2-hydroxyaryl thiazolines are known to be stabilized electronically and by intramolecular H-bonding from phenolic OH to thiazoline (*57*), so ring opening to the amide would be slowed. This alternate pathway (A) could account for the sequence motif differences of the condensation/cyclization domains in HMWP2 as compared to the typical nonribosomal peptide synthetase condensation domain (Table 3). The sequence HHxxxDG (core motif 3) (*31*) has been identified as critical for amide-bond formation by sequence analysis (*58*) as well as mutational study (*59*, *60*). The second histidine is believed to serve as a base catalyst for deprotonation of the NH_3^+ form of the aminoacyl-S-PCP nucleophiles prior to amide bond formation (*58*), and its mutation to valine abolishes dipeptide formation in vitro in a gramicidin S/tyrocidine synthetase system (*59*). The *Bacillus licheniformis* bacitracin synthetase, *Yersinia* HMWP2 and HMWP1, and the *V. anguillarum* AngR protein involved in anguibactin biosynthesis, all enzymes catalyzing biosynthesis of a product containing thiazoline rings, retain only the conserved aspartate residue of the HHxxxDG motif (Table 3). An open reading frame in *Mycobacterium tuberculosis* (MTCY22H8.02) has also been noted with a similar core 3 sequence (*33*) (Table 3), and its gene product is presumed to be involved in the biosynthesis of mycobactin (L. Quadri, P. Weinreb, C. T. W., unpublished observations), an oxazoline-containing siderophore (*61*). For heterocyclization by pathway A (Figure 8), the attacking nucleophile would not be an α-amino group but rather the thiolate or alkoxide side chain of cysteine, serine, or threonine-S enzymes. The conserved aspartate and serine residues in the cyclization domains (Table 3) are candidates for mutagenesis to determine whether amide bond formation and/or cyclodehydration steps are differentially affected in an attempt to distinguish between pathways A and B of Figure 8.

Demonstration of the heterocyclization capacity of HMWP2 1−1491, the first for a nonribosomal peptide synthetase enzyme, supports the hypothesis of Konz et al. (*33*) who described a putative thiazoline-ring forming domain in the bacitracin synthetase. By extension, we anticipate that the second condensation/cyclization domain of HMWP2 (residues 1492−1926) will have the same catalytic properties, adding a second thiazoline ring to the yersiniabactin precursor and giving HPTT-COOH. HMWP1, whose sequence is reported for *Y. enterocolitica* (*23*), contains polyketide synthase domains as well as one more cyclization/condensation domain and would presumably be responsible for the synthesis of the remainder of yersiniabactin from malonyl coenzyme A, S-adenosylmethionine, and an additional cysteine residue. Having demonstrated the capacity of HMWP2 1−1491 to adenylate cysteine, to be loaded on its carrier protein domains with salicylate and cysteine, and to catalyze condensation/heterocyclization to give HPT-COOH, we are poised to address the functions of the remainder of HMWP2 as well as HMWP1. This enzymology, once deconvoluted, may be a prime target for antiyersinial strategies in antibiotic discovery and more generally for blockade of other thiazoline and oxazoline-containing siderophores that are virulence factors in, for example, *Vibrio* species (anguibactin, vibriobactin) and *P. aeruginosa* (pyochelin) (*3*). Likewise, the biogenesis of heterocyclic-containing nonribosomal peptide antibiotics such as bacitracin and bleomycin probably employ an equivalent enzymatic strategy for heterocycle construction.

ACKNOWLEDGMENT

We thank Scott Bearden and Jackie Fetherston for their help in the initial construction of some *ybtE* and *irp2* subclones. We also thank Torsten Stachelhaus for helpful discussions.

REFERENCES

1. Jackson, S. and Burrows, T. W. (1956) *Br. J. Exp. Pathol. 37*, 577−583.
2. Robins-Browne, R. M. and Prpic, J. K. (1985) *Infect. Immun. 47*, 774−779.
3. Griffiths, E. (1987) in *Iron and Infection: Molecular, Physiological and Clinical Aspects* (Bullen, J. J. and Griffiths, E., Eds.) pp 1−25, 69−137, John Wiley & Sons, Chichester, Great Britian.
4. Neilands, J. B. (1981) *Annu. Rev. Biochem. 50*, 715−731.
5. Heesemann, J. (1987) *FEMS Microbiol. Lett. 48*, 229−233.
6. Haag, H., Hantke, K., Drechsel, H., Stojiljkovic, I., Jung, G., and Zähner, H. (1993) *J. Gen. Microbiol. 139*, 2159−2165.
7. Chambers, C. E. and Sokol, P. A. (1994) *J. Clin. Microbiol. 32*, 32−39.

8. Drechsel, H., Stephan, H., Lotz, R., Haag, H., Zähner, H., Hantke, K., and Jung, G. (1995) *Liebigs Ann. 1995*, 1727−1733.
9. Chambers, C. E., McIntyre, D. D., Mouck, M., and Sokol, P. A. (1996) *BioMetals 9*, 157−167.
10. Cox, C. D., Rinehart, K. L., Jr., Moore, M. L., and Cook, J. C., Jr. (1981) *Proc. Natl. Acad. Sci. U.S.A.* 78, 4256−4260.
11. Jalal, M. A. F., Hossain, M. B., van der Helm, D., Sanders-Loehr, J., Actis, L. A., and Crosa, J. H. (1989) *J. Am. Chem. Soc. 111*, 292−296.
12. Yamamoto, S., Okujo, N., and Sakakibara, Y. (1994) *Arch. Microbiol. 162*, 249−254.
13. Griffiths, G. L., Sigel, S. P., Payne, S. M., and Neilands, J. B. (1984) *J. Biol. Chem. 259*, 383−385.
14. Fetherston, J. D. and Perry, R. D. (1994) *Mol. Microbiol. 13*, 697−708.
15. Rakin, A., Urbitsch, P., and Heesemann, J. (1995) *J. Bacteriol. 177*, 2292−2298.
16. Carniel, E., Guilvout, I., and Prentice, M. (1996) *J. Bacteriol. 178*, 6743−6751.
17. Buchrieser, C., Prentice, M., and Carniel, E. (1998) *J. Bacteriol. 180*, 2321−2329.
18. Perry, R. D. and Fetherston, J. D. (1997) *Clin. Microbiol. Rev. 10*, 35−66.
19. Fetherston, J. D., Lillard, J. W., Jr., and Perry, R. D. (1995) *J. Bacteriol. 177*, 1824−1833.
20. Bearden, S. W., Fetherston, J. D., and Perry, R. D. (1997) *Infect. Immunol. 65*, 1659−1668.
21. Rakin, A., Saken, E., Harmsen, D., and Heesemann, J. (1994) *Mol. Microbiol. 13*, 253−263.
22. Guilvout, I., Mercereau-Puijalon, O., Bonnefoy, S., Pugsley, A. P., and Carniel, E. (1993) *J. Bacteriol. 175*, 5488−5504.
23. Pelludat, C., Rakin, A., Jacobi, C. A., Schubert, S., and Heesemann, J. (1998) *J. Bacteriol. 180*, 538−546.
24. Gehring, A. M., Bradley, K. A., and Walsh, C. T. (1997) *Biochemistry 36*, 8495−8503.
25. Gehring, A. M., Mori, I., and Walsh, C. T. (1998) *Biochemistry 37*, 2648−2659.
26. Fetherston, J. D., Schuetze, P., and Perry, R. D. (1992) *Mol. Microbiol. 6*, 2693−2704.
27. Gill, S. C. and von Hippel, P. H. (1989) *Anal. Biochem. 182*, 319−326.
28. Lambalot, R. H., Gehring, A. M., Flugel, R. S., Zuber, P., LaCelle, M., Marahiel, M. A., Reid, R., Khosla, C., and Walsh, C. T. (1996) *Chem. Biol. 3*, 923−936.
29. Bergeron, R. J., Wollenweber, M., and Wiegand, J. (1994) *J. Med. Chem. 37*, 2889−2895.
30. Hoveyda, H. R., Karunaratne, V., and Orvig, C. (1992) *Tetrahedron 48*, 5219−5226.
31. Marahiel, M. A., Stachelhaus, T., and Mootz, H. D. (1997) *Chem. Rev. 97*, 2651−2673.
32. Kagan, R. M. and Clarke, S. (1994) *Arch. Biochem. Biophys. 310*, 417−427.
33. Konz, D., Klens, A., Schörgendorfer, K., and Marahiel, M. A. (1997) *Chem. Biol. 4*, 927−937.
34. Gillet, S., Hountondji, C., Schmitter, J.-M., and Blanquet, S. (1997) *Protein Sci. 6*, 2426−2435.
35. Carmi, R., Carmeli, S., Levy, E., and Gough, F. J. (1994) *J. Nat. Prod. 57*, 1200−1205.
36. Carniel, E., Mazigh, D., and Mollaret, H. H. (1987) *Infect. Immunol. 55*, 277−280.
37. Carniel, E., Antoine, J.-C., Guiyoule, A., Guiso, N., and Mollaret, H. H. (1989) *Infect. Immunol. 57*, 540−545.
38. Carniel, E., Mercereau-Puijalon, O., and Bonnefoy, S. (1989) *Infect. Immunol. 57*, 1211−1217.
39. de Almeida, A. M. P., Guiyoule, A., Guilvout, I., Iteman, I., Baranton, G., and Carniel, E. (1993) *Microb. Pathog. 14*, 9−21.
40. Carniel, E., Guiyoule, A., Mercereau-Puijalon, O., and Mollaret, H. H. (1991) *Contrib. Microbiol. Immunol. 12* , 192−197.
41. Carniel, E., Guiyoule, A., Guilvout, I., and Mercereau-Puijalon, O. (1992) *Mol. Microbiol. 6*, 379−388.
42. Young, G. M., and Miller, V. L. (1997) *Mol. Microbiol. 25*, 319−328.
43. Wake, A., Misawa, M., and Matsui, A. (1975) *Infect. Immun. 12*, 1211−1213.
44. Galimand, M., Guiyoule, A., Gerbaud, G., Rasoamanana, B., Chanteau, S., Carniel, E., and Courvalin, P. (1997) *New Engl. J. Med. 337*, 677−680.
45. Stubbe, J. and Kozarich, J. W. (1987) *Chem. Rev. 87*, 1107−1136.
46. Bollag, D. M., McQueney, P. A., Zhu, J., Hensens, O., Koupal, L., Liesch, J., Goetz, M., Lazarides, E., and Woods, C. M. (1995) *Cancer Res. 55*, 2325−2333.
47. Floss, H. G. and Beale, J. M. (1989) *Angew. Chem., Int. Ed. Engl. 28*, 146−177.
48. Selva, E., Beretta, G., Montanni, N., Saddler, G. S., Gastaldo, L., Ferrari, P., Lorenzetti, R., Landini, P., Ripamonti, F., Goldstein, B. P., Berti, M., Montanaro, L., and Denaro, M. (1991) *J. Antibiot. 44*, 693−701.
49. Elbein, A. D. (1984) *CRC Crit. Rev. Biochem. 16*, 21−49.
50. Yorgey, P., Lee, J., Kördel, J., Vivas, E., Warner, P., Jebaratnam, D., and Kolter, R. (1994) *Proc. Natl. Acad. Sci. U.S.A. 91*, 4519−4523.
51. Li, Y.-M., Milne, J. C, Madison, L. L., Kolter, R., and Walsh, C. T. (1996) *Science 274*, 1188−1193.
52. Reichert, J., Sakaitani, M. and Walsh, C. T. (1992) *Protein Sci. 1*, 549−556.
53. Pieper, R., Haese, A., Schröder, W., and Zocher, R. (1995) *Eur. J. Biochem. 230*, 119−126.
54. Burmester, J., Haese, A., and Zocher, R. (1995) *Biochem. Mol. Biol. Intl. 37*, 201−207.
55. Weber, G., Schörgendorfer, K., Schneider-Scherzer, E., and Leitner, E. (1994) *Curr. Genet. 26*, 120−125.
56. Conti, E., Stachelhaus, T., Marahiel, M. A., Brick, P. (1997) *EMBO J. 16*, 4174−4183.
57. Hoveyda, H. R. (1993), University of British Columbia, Ph.D. Thesis.
58. de Crécy-Lagard, V., Marlière, P., and Saurin, W. (1995) *C. R. Acad. Sci., Ser. III 318*, 927−936.
59. Stachelhaus, T., Mootz, H. D., Bergendahl, V., and Marahiel, M. A. (1998) *J. Biol. Chem.*, in press.
60. Vater, J., Stein, T., Vollenbroich, D., Kruft, V., Wittmann-Liebold, B., Franke, P., Liu, L., and Zuber, P. (1997) *J. Protein Chem. 16*, 557−564.
61. Barclay, R., Ewing, D. F., and Ratledge, C. (1985) *J. Bacteriol. 164*, 896−903.

BI9812571